

Artist depiction of a protoplanetary disk. Image Credit: NASA

# Spectro-Astrometry of Molecular Emission in DR Tauri

Logan R. Brown, Matthew R. Troutman, Erika L. Gibb  
University of Missouri – St. Louis



## ABSTRACT

To understand how life originated on Earth, we must investigate how the necessary water and other prebiotic molecules were distributed through the protoplanetary disk from which the solar system formed. To infer this, we study analogs to the early solar system: T Tauri stars. These objects are low-mass, pre-main sequence stars surrounded by circumstellar disks of material from which planets are believed to form. How water is distributed through a protoplanetary disk is of particular interest. We present high-resolution, near-infrared spectro-astrometric data for the T Tauri star DR Tau using NIRSPEC at the Keck II telescope. Spectro-astrometry obtains sub-seeing spatial information from emission lines originating in a non-point source object, such as a circumstellar disk. We report the first detection of water spectro-astrometric signatures in a protoplanetary disk. Three water features near 3  $\mu\text{m}$  were averaged together to produce the total signal analyzed. Using a disk model, we constrained the position angle of the disk ( $\sim 140^\circ$ ), the inclination of the disk ( $\sim 13^\circ$ ), and the emitting region of the water emission lines ( $\sim 0.056 - 0.38$  AU). Furthermore, we attempted to constrain the emitting region for observed OH emission.

## DISK BACKGROUND

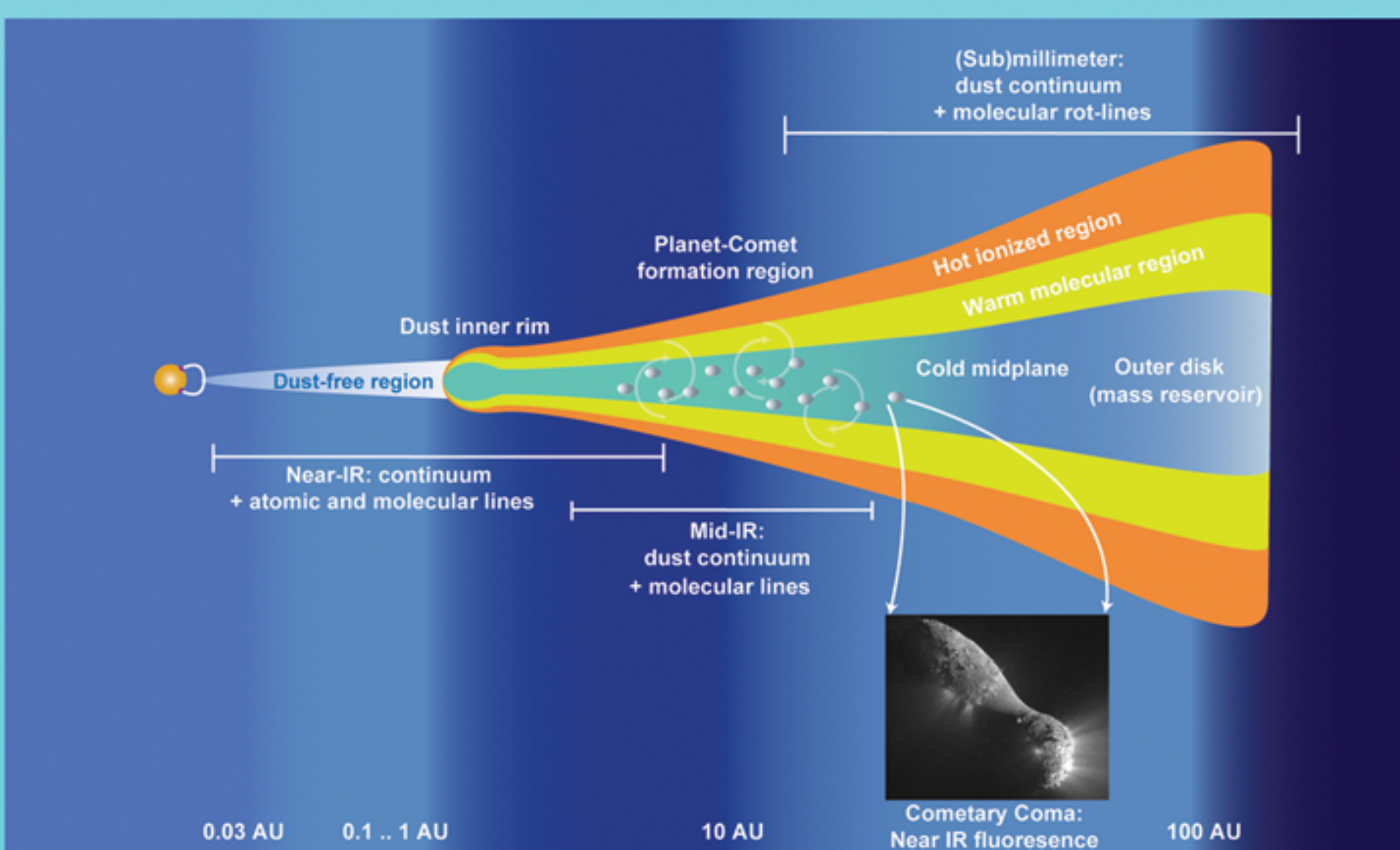


Figure 1 - Image courtesy Geronimo Villanueva, NASA Goddard Space Flight Center

Protoplanetary disks have masses on the order of tens of Jupiter masses, extend outward to about 100 AU, and have a flared geometry, a depiction of which is found in figure 1. Disks have three main regions characterized by the chemical processes found within (Walsh et. al. 2010):

- The **cold midplane** is a cold dense region where molecules freeze onto dust grains.
- In the **warm molecular layer**, molecular synthesis is stimulated by increasing temperatures and the evaporation of molecules from dust grains.
- Stellar and cosmic radiation dissociates and ionizes molecules into constituent radicals, atoms, and ions in the **hot ionized disk atmosphere**.

## OBSERVATIONS & ANALYSIS

The data were reduced with a standard method, involving flat fielding, dark subtraction, and calibration using a standard star. The raw frames are cropped, cleaned of hot and dead pixels, and spatially and spectrally aligned. Getting a spectrum for the emission coming from the disk allows us to then analyze features in to find the spatial extent of emission using a technique called spectroastrometry. Spectro-astrometry measures the wavelength dependence of the position of an object. Adopting the method of Pontoppidan et. al. (2008), we performed a Gaussian fit to each beam in the observation, summed up in frequency space, the centroid of which is then assumed to be the centroid of the star. By measuring the “center-of-light” in each velocity bin, the spatial offset was determined, thus producing the spectroastrometric (SA) signal. For each pixel in frequency space, the “center-of-light” is found as follows:

$$X_v = C \frac{\sum_i (x_i(v) - x_0) F_i(v)}{\sum_i F_i(v)}, \quad [\text{pixels}]$$

$X_v$  is the spatial offset (the spectro-astrometric signal),  $x_i$  is the location of a pixel,  $x_0$  is the centroid of the star, and  $F_i$  is the flux contained in the pixel at location  $x_i$ .  $C$  is a correction factor in order to account for the fact that all the flux might not be included in the window over which the signal is calculated and is a number of order unity. In order to interpret the signal, a model of the source is needed.

## MODELING

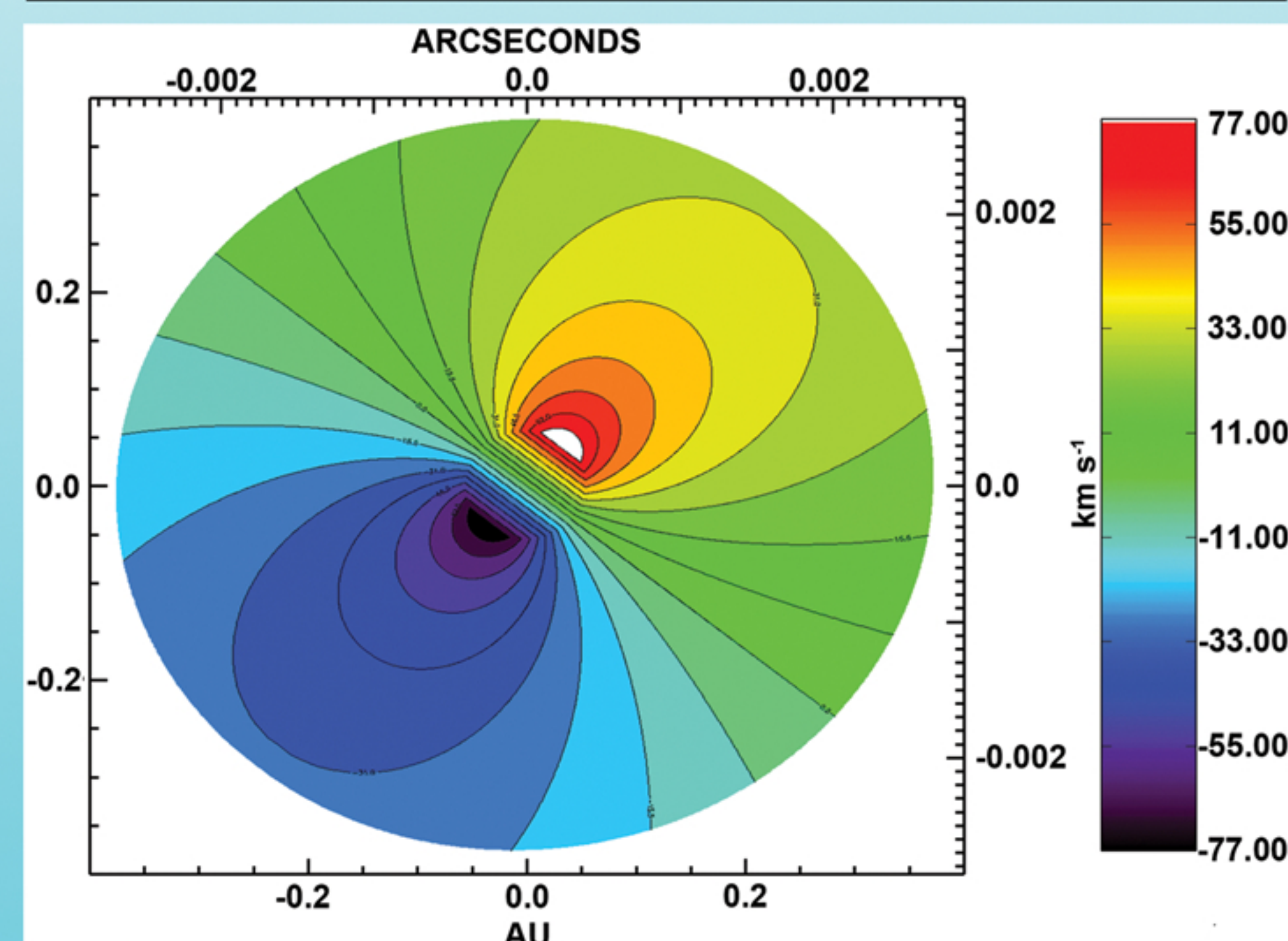


Figure 2 - Example of a modeled disk with velocity contours indicated.

Comparing the model to the calculated signal allows us to determine the spatial extent of emission and the geometry of the object. In modeling the disk, we assume:

- Flat, circular slab.
- Constant radial surface density.
- Disk material rotates with simple Keplerian motion (material closer to the center will be moving faster than material further away).

An adaptive mesh was used to divide the modeled disk into pieces such that any radial step or angular step moves no more than a set model resolution in velocity space. An emitted flux is calculated for each little chunk of the disk, assuming each to be their own separate black body:

$$F = (\text{Area}) T^4$$

The temperature varies as  $R^{-3/4}$  so that the flux will vary as  $R^{-3}$ . The calculated fluxes are then normalized by the calculated flux of the star. Having this modeled disk flux, we can then make an artificial spectra from which we can calculate an SA signal as outlined above. An example of a modeled disk can be found in figure 3.

From there, an inner and outer radius of emission, inclination, and position angle on the sky are varied to find a signal that best matches the one calculated from the data. A least chi squared comparison is used to determine which model is the best fit:

$$\chi^2 = \sum_{i=1}^n \frac{(O_i - E_i)^2}{E_i}$$

The inner and outer radius that generates the best fit is then the spatial extent of emission for that feature. Figure 3 shows our results, a plot of the SA signals and fitted model. Figure 4 shows a contour plot of the least chi squared values with differing emitting regions and holding all other variable constant. The table below shows a summary of the best fit parameters:

SUMMARY OF MODEL PARAMETERS

Beta <sup>1</sup>	P.A. <sup>2</sup> (°)	Inc. <sup>3</sup> (°)	Mass <sup>4</sup> (M <sub>⊙</sub> )	R <sub>in</sub> (AU)	R <sub>out</sub> (AU)
3	140	13	0.4	0.056	0.38

NOTE. - (1) Mandel et al. 2012. (2) PA is degrees east of north. (3) Inc is such that 0° is face on, 90° is edge on. (4) Isella et al. 2009.

## RESULTS

SA analysis, in addition to spectroscopic modeling and protoplanetary disk chemical modeling of others, suggest a scenario in which we observed hot water emission from the disk atmosphere above the inner, terrestrial planet region of a protoplanetary disk. In addition to water, OH was identified but did not give any structure in the SA signal. Preliminary work in fitting a modeled SA signal to the error envelope of the OH features suggests an upper limit of the emitting region being approximately 0.2 AU.

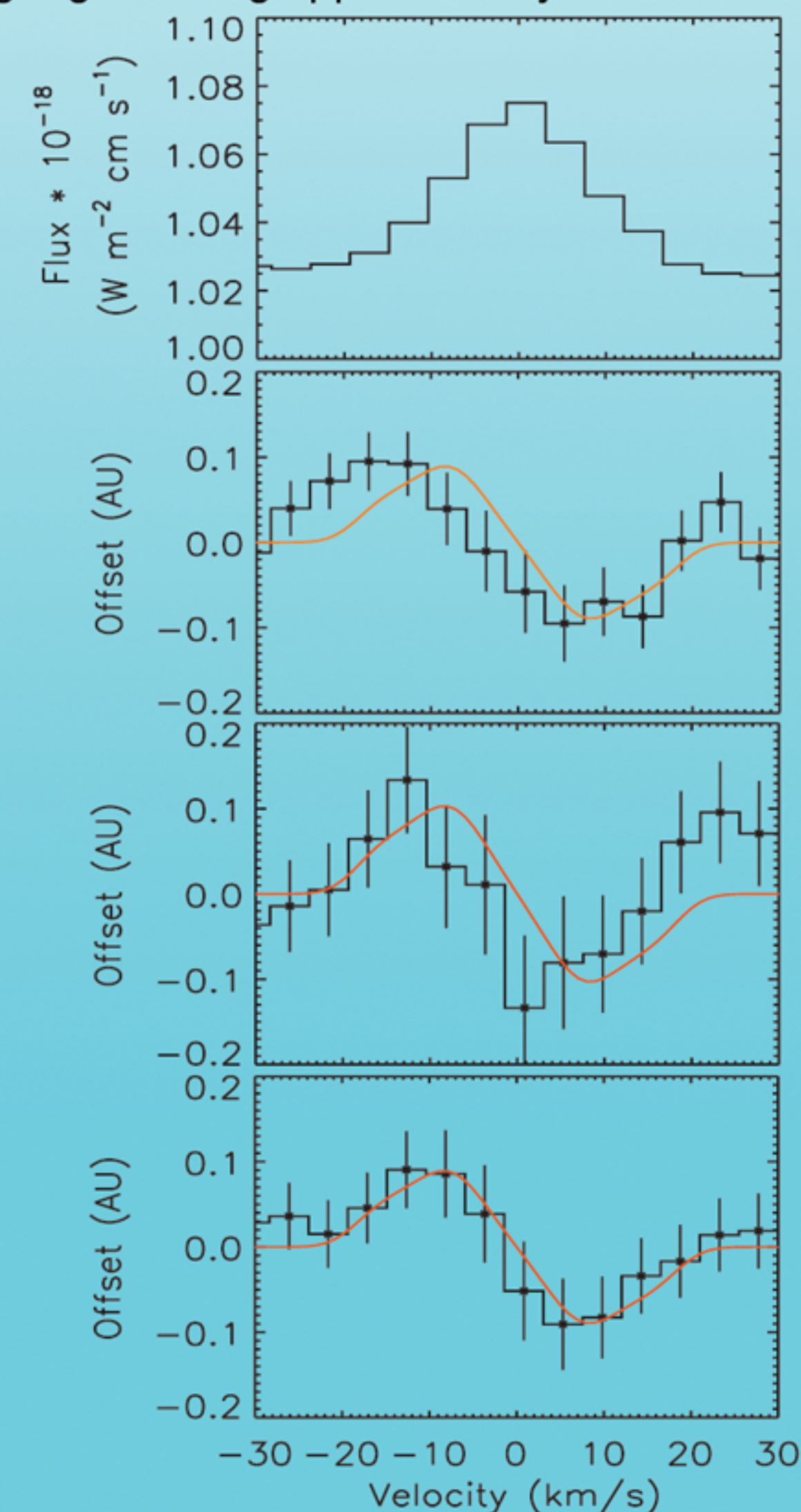


Figure 3 - The top panel shows the average emission profile in velocity space of three H<sub>2</sub>O 001 – 000 vibrational transition lines that gave clear spectro astrometric signals. The bottom three panels are the averaged SA signals for those features (black line) for each slit PA and 180 offset with the best-fit model over plotted (red line). The horizontal axis is in velocity space (km s<sup>-1</sup>).

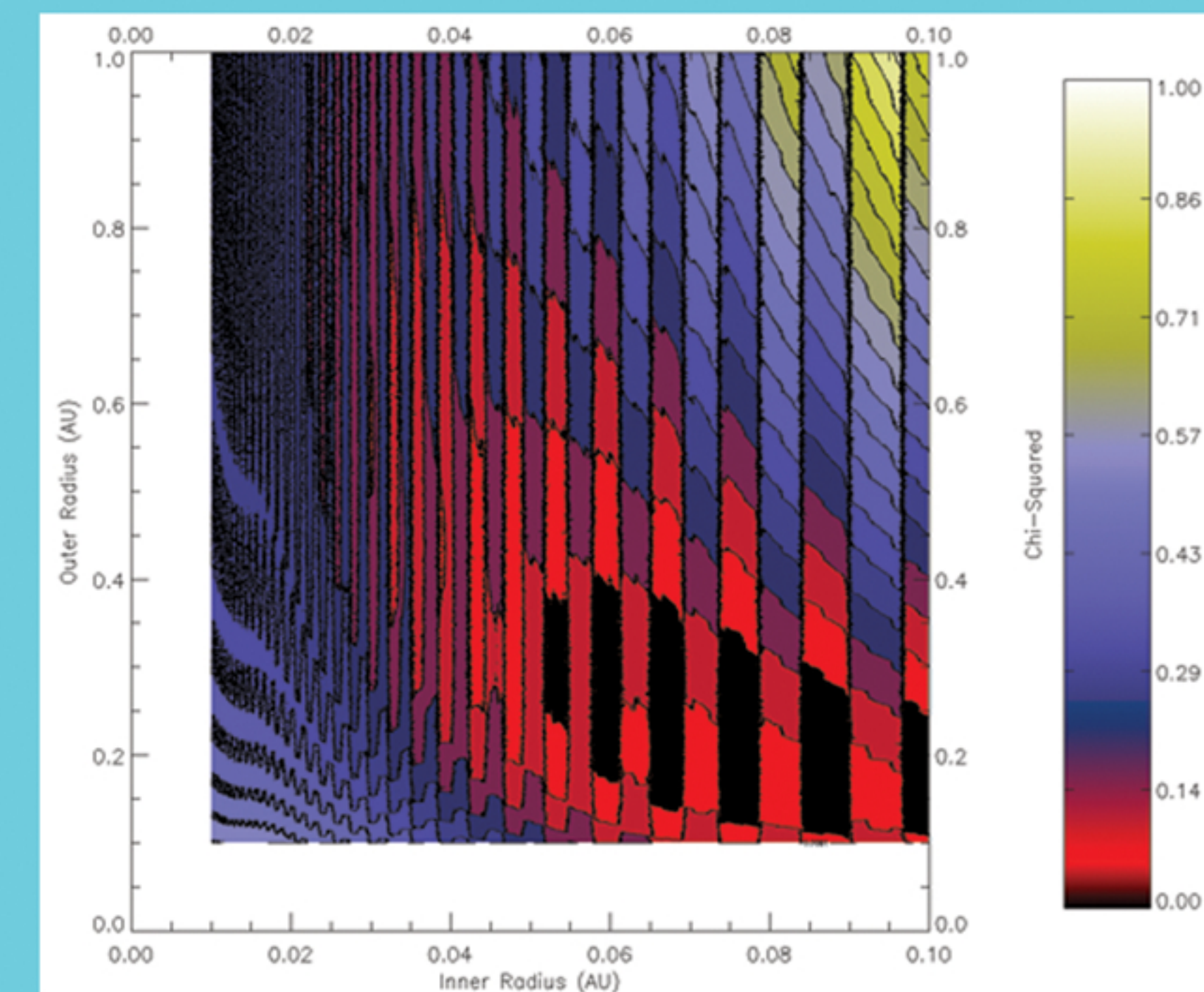


Figure 4 - A contour plot of the least chi squared values. Inner and Outer emitting radius was varied, all other values held constant.

## ACKNOWLEDGEMENTS

LRB, MRT, and ELG gratefully acknowledge support from NSF's Stellar Astronomy program and the American Recovery and Reinvestment Act of 2009 (NSF 0908230), JPL (RSA No: 1423736), and the NASA Exobiology and Evolutionary Biology program (NNX07AK38G). We also acknowledge the contributions made by undergraduate research assistants Bryant Dentinger and Nick Kraftor. Data presented herein were obtained at the W. M. Keck Observatory, which is operated as a scientific partnership among the California Institute of Technology, the University of California, and the National Aeronautics and Space Administration. The Observatory was made possible by the generous financial support of the W. M. Keck Foundation. The authors recognize and acknowledge the very significant cultural role and reverence that the summit of Mauna Kea has always had within the indigenous Hawaiian community.

## REFERENCES

- Isella, A., Carpenter, J. M., & Sargent, A. I. 2009, ApJ, 701, 260  
Mandell, A. M., Bast, J., van Dishoeck, E. F., et al. 2012 ApJ, 747, 92  
Pontoppidan, K. M., Blake, G. A., van Dishoeck, E. F., Smette, A., Ireland, M. J., & Brown J. 2008 ApJ, 684, 1323  
Brown J. 2008 ApJ, 684, 1323  
Salyk, C. et al. 2008, ApJ, 676, 49  
Walsh, C., Miller, T. J., & Nomura, H. 2010 ApJ, 722, 1607